

# SuperCIC: enhanced winding current density for hybrid windings of tokamaks

P. McIntyre, *Member, IEEE*, J. Breitschopf, T.E. Brown, D. Chavez, J.N. Kellams, and A. Sattarov

**Abstract**— The design is presented for a new approach to cable-in-conduit (SuperCIC) for use in the high-field windings of tokamaks. Two layers of high-field superconductor wires are cabled onto a thin-wall perforated center tube. An overwrap is applied and the cable is inserted as a loose fit into a sheath tube. The sheath tube is drawn down onto the cable to compress the wires onto the center tube and immobilize them. The SuperCIC is then co-wound with a high-strength armor extrusion, which is kerf-cut so that the co-winding onto a coil mandrel can be made without deformation within the armor or the CIC.

SuperCIC facilitates hybrid windings, in which sub-windings of NbTi are used where  $B < 7$  T, Nb<sub>3</sub>Sn where  $B < 14$  T, and Bi-2212 where  $B > 14$  T to minimize superconductor cost. Demountable splices are used to interconnect layers. A conceptual design has been prepared for a tokamak with aspect ratio  $A \sim 2.0$ , magnetic field of 17.4 T at the inner windings and 6.7 T at the plasma, and winding current density  $\sim 140$  A/mm<sup>2</sup> - sufficient for optimizing the fusion power density in a compact spherical tokamak.

**Index Terms**—superconducting cable, hybrid windings, tokamak, fusion

## I. INTRODUCTION

Magnetic confinement fusion requires a magnetic field distribution to confine a plasma while it is heated and undergoes fusion. Several magnetic field geometries have been developed in previous decades: tokamak [1,2], mirror configuration [3], and stellerator [4]. In the present day ITER is 50% complete, JET is operational, and GOL-NB and Wendelstein 7-X are operating.

A new generation of ambitious projects is being developed, including two compact tokamaks [5,6] and a mirror-geometry system [7]. Fig. 1 shows the conceptual design for each project. All three initiatives are driven by the need for increasing the magnetic field strength in the confinement system to sustain the combination of density, temperature, and confinement time that would be required for a fusion power system. Each initiative is motivated by the recent development of high-current REBCO-based cables [8], and its capability to carry high current in high magnetic field at an operating temperature of 30-40 K.

The NbTi SuperCIC was developed under funding from the US Dept. of Energy, grants DE-SC0017205 and DE-SC0015198.

P.M. McIntyre and A. Sattarov are with the Accelerator Research Center, Texas A&M University, College Station, TX 77845 USA and also with Accelerator Technology Corp. College Station, TX 77845 USA (email: [p-mcintyre@tamu.edu](mailto:p-mcintyre@tamu.edu)).

J. Breitschopf is now with the Department of Physics, Colorado State University, Fort Collins CO. 80526. (email: [jeff.breitschopf@gmail.com](mailto:jeff.breitschopf@gmail.com)).

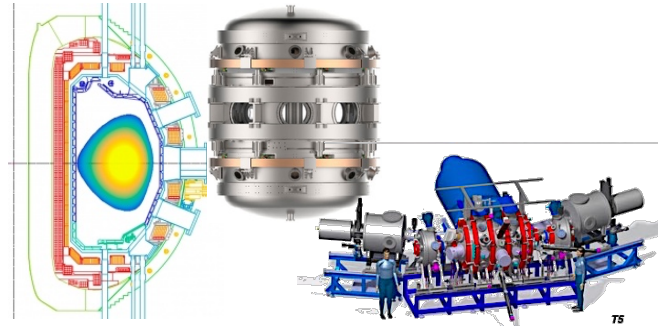


Fig. 1. Three new initiatives for compact high-field magnet configurations for fusion: DIII-D tokamak; TE tokamak, LMA mirror.

But REBCO superconducting tape is extremely expensive. The performance of REBCO tapes has improved considerably in recent years, but the price has not reduced. There is thus the potential for major advancement in magnetic fusion with higher magnetic field that has not been possible with conventional superconductors, but there is frustration with the extreme cost for the new REBCO-based cables. Those considerations motivated us to develop a conceptual design for high-field magnet configurations for fusion based upon a new technology for advanced cable-in-conduit (SuperCIC) that we have developed for an accelerator application.

As a further context, Menard [9] has evaluated the importance of the current density  $J_{WP}$  of the toroidal field coil (TF) winding pack and the device aspect ratio  $A$ . Fig. 2 (reproduced from Fig. 5 of Ref. 9) shows the dependence of net electric power of a tokamak upon those two parameters. For the scan in Fig. 2 the plasma major radius is held fixed at 3 m and the plasma is assumed to have full non-inductive current sustainment provided by a bootstrap current and a neutral beam current drive. Ref. 9 presents the interplay of the many parameters that lead to the limits on  $P_{net}$ : “For ITER-like magnet parameters of maximum field in windings  $B_{max} \approx 12$  T and  $J_{WP} = 20$  MA/m<sup>2</sup>, the fusion gain  $Q_{DT}$  is constrained to be less than 3 while the engineering gain is  $Q_{eng} \leq 0.5$ . Increasing  $B_{max}$  from 12 T to 19 T increases  $Q_{DT}$  to above 4, but  $Q_{eng}$  remains

D. Chavez is now with Department da Fisica, Universidad Guanajuato, Leon, MX.

J.N. Kellams is now with Lockheed Martin Aeronautics, Palmdale, CA. 93599 USA (email: [jnkellams@tamu.edu](mailto:jnkellams@tamu.edu))

T. Brown is with Princeton Plasma Physics Lab, Princeton, NJ 08540 USA (email: [tbrown@pppl.gov](mailto:tbrown@pppl.gov))

Color versions of the figures are available online at <http://ieeexplore.ieee.org>. Digital Object Identifier will be inserted here upon acceptance.

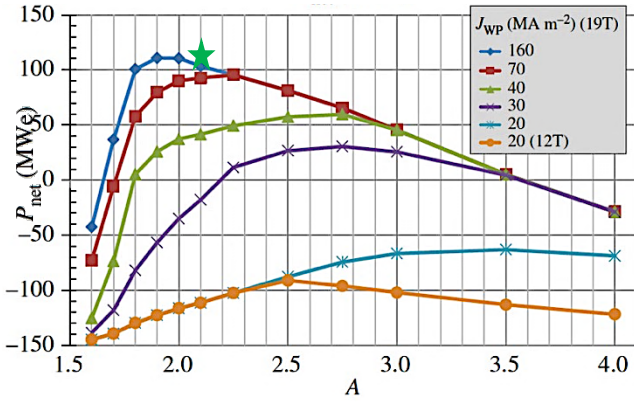


Fig. 2. Dependence of the net electric power from a tokamak as a function of its aspect ratio  $A$  and the winding package current density  $J_{WP}$ . The green star indicates the parameters for PPPL’s spherical tokamak design using SuperCIC windings. (from Ref. 9)

less than unity. However, for  $B_{max} \approx 19$  T and  $J_{WP} = 30$  MA m<sup>-2</sup>, the fusion gain increases by a factor of 2 and  $Q_{eng} \geq 1$  between  $A = 2.2$  and 3.5. As shown in Fig. 2, as the winding pack current density is further increased, lower aspect ratio solutions produce the highest fusion power and net electric power with  $P_{fusion}$  up to 600 MW and  $P_{net} > 100$  MWe”.

These trends indicate that lower aspect ratio tokamaks benefit the most from increased JWP in the TF magnet system. While the limits on higher aspect ratio are to some extent model-dependent in Menard’s analysis, the importance of high current density in the winding pack is not. The Nb<sub>3</sub>Sn ITER toroids have a current density  $J_{WP} = 20$  MA/m<sup>2</sup>, insufficient to yield any net electric power from fusion for any aspect ratio in a compact R=3 m device.

Two recent developments are significant for these two critical parameters. First, PPPL has developed a design for a spherical tokamak Fig. 3 with aspect ratio  $A \sim 2.0$ , suitable for studies of liquid metal diverter and first wall [10]. Second, The SuperCIC coil technology reported in this paper provides a basis for toroid and solenoid windings with  $J_{WP} \sim 140$  MA/m<sup>2</sup>. The green star in Fig. 2 shows that a tokamak embodying those developments would have the potential for optimum performance as a fusion energy system.

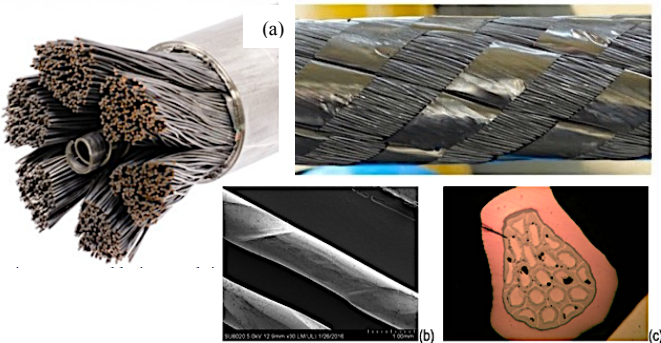


Fig. 4. a) wire bundle within an ITER TX cable; b) extracted wires from the cable, showing indentations where wires are compacted against one another; c) cross-section showing damaged microstructure [11].

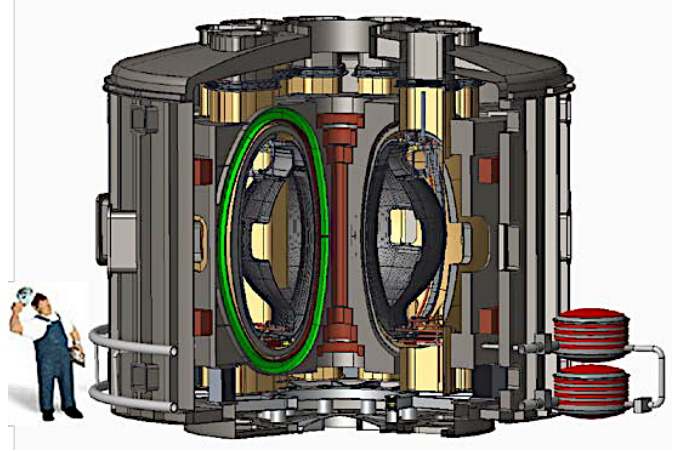


Fig. 3. Toroidal confinement facility to study liquid metal systems within a spherical tokamak (from Ref. 10).

## II. LIMITATIONS OF CONVENTIONAL CIC CONDUCTORS

The magnet windings of a tokamak pose a central challenge for enhancing performance, reducing cost and risk for magnetic confinement fusion systems. In conventional armored cable-in-conduit (CIC) for tokamaks, Nb<sub>3</sub>Sn/Cu wires are formed into a ‘rope-of-ropes’ configuration with a flexible center tube and then compressed within an armor sheath, as shown in Fig. 4a. The compression in the sheath within the armor forms severe indents in the strand cross-section [11] (Fig. 4c). Strand performance is also reduced by the compressive strain due to differential thermal contraction during cooldown, since the wire package is friction-locked to the armor. Further degradation from cyclic loading (ramp up and down of current in presence of magnetic field) is most likely related to unsupported wire segments within each rope. The result is that such CIC conductors operate with less than half of the wire current density that the native wires would have individually. The CIC windings for both toroid and solenoid windings of ITER have  $J_{WP} \sim 20$  A/mm<sup>2</sup>, even though ITER-grade Nb<sub>3</sub>Sn wire has an average current density  $J_e = 380$  A/mm<sup>2</sup> @ 12 T, 4.2 K, 0.1 μV/cm [12], and HyperTech’s tube-process Nb<sub>3</sub>Sn wire [13] has  $J_e = 780$  A/mm<sup>2</sup> @ 12 T, 4.2 K, 0.1 μV/cm with even better AC loss performance.

A collaboration of Texas A&M University (TAMU), Accelerator Technology (ATC), and HyperTech Research have developed a new approach to the cable technology and coil technology for CIC [14], shown in Fig. 5a. All superconducting wires are supported uniformly, the cable structure provides stress management at the cable level, and armor structure is co-wound with the cable as the layers of the winding are formed. As discussed below, the ‘SuperCIC’ technology eliminates indentation of wires and provides uniform support of all wires within the cable over its full length. It also eliminates friction-lock of the cable to its center tube and sheath, and so eliminates compressive strain from cooldown and bending strain from coil-forming. It thus makes it possible to preserve the native performance of the superconducting wires within a high-current armored cable in a high-field winding. The

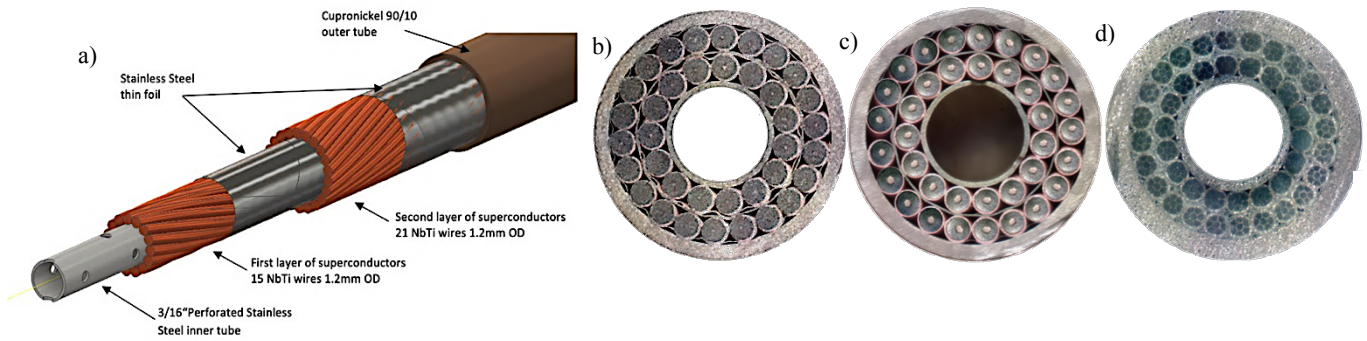


Fig. 5. a) cut-away detail of two-layer Super-CIC; cross-sections of 2-layer SuperCIC using b) fine-filament NbTi/Cu; c) tube-process Nb<sub>3</sub>Sn/Cu; d) Bi-2212.

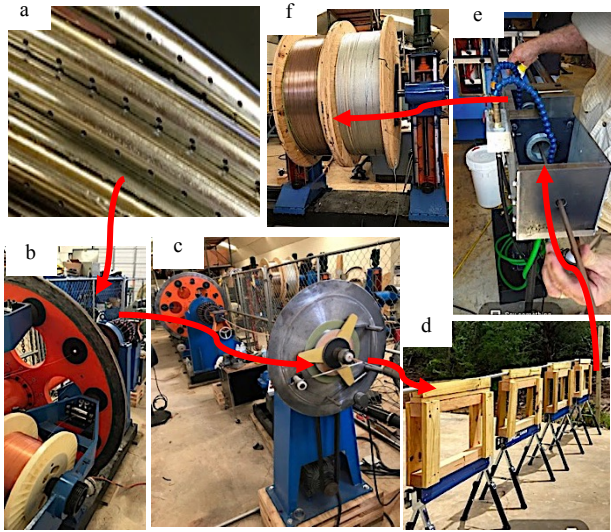


Fig. 6. Fabrication of SuperCIC: a) perforated center tube; b) cable superconducting wires onto center tube, c) apply foil over-wrap; d) pull straight 150 m cable through sheath tube with loose fit; repeat b-d for the second layer; e) draw sheath tube onto cable.

preservation of wire performance gives two benefits: the magnetic systems require less superconductor and so are less expensive; and the space required for the windings is greatly reduced, so more aperture is available for the optimization of the fusion tokamak.

### III. SUPER-CIC CABLE TECHNOLOGY

The SuperCIC fabrication sequence is illustrated in Fig. 6. The superconducting wires are cabled with a twist pitch around a perforated thin-wall center tube of stainless steel (Fig. 6a,b). A thin-foil tape overwrap is applied with opposite twist pitch (Fig. 6c). The above sequence is repeated to cable a second layer of superconducting wires for the 2-layer SuperCIC required for the HE-LHC dipole windings. The cable is then pulled through a sheath tube (Fig. 6d), and the sheath tube is drawn down upon the cable (Fig. 6e) to compress the wires against the center tube and immobilize them. Fig. 5 shows cross-sections of completed 2-layer CIC.

The thin-wall 316L center tube provides several important functions. First, it provides stress management at the cable level. Fig. 7a shows finite element (FEA) simulation of the compression of the wire and center tube when the sheath tube is drawn down onto the cable. The center tube deflects

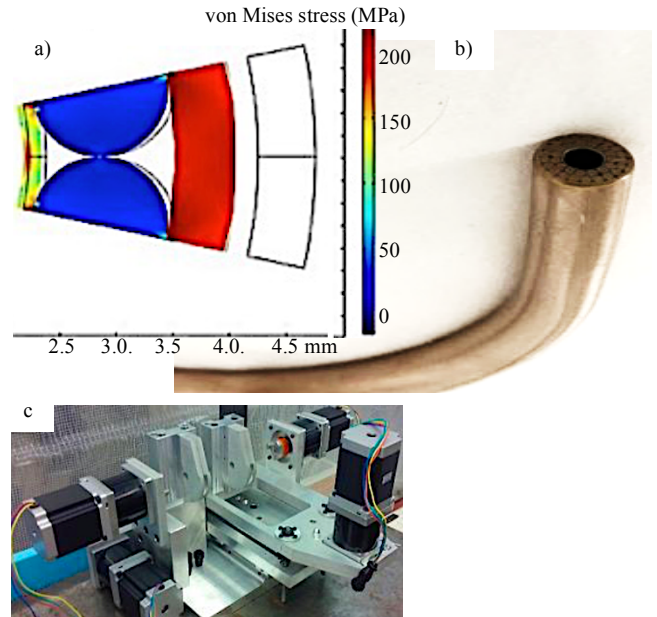


Fig. 7. a) FEA modeling of compression of sheath tube to immobilize strands. Strain is expanded x1000 to show how thin-wall center tube deforms to preload all wires to manage stress within the CIC. b) segment of a 2-layer SuperCIC formed into a U-bend with a bend radius of 3 cm – only 8 times greater than the CIC radius. c) Robotic bend tool that forms a constant-radius bend while keeping the CIC round in cross-section throughout.

elastically as each wire is compressed against it, so the wires are immobilized (so they cannot move under Lorentz forces), but they are protected from strain by the elastic support from the center tube. Second, the perforations of the center tube provide fluid connection between the hollow interior of the center tube and the void spaces among the wires. The enthalpy of the liquid helium contacting the wire surfaces provides valuable stabilization against growth of micro-quenches.

The twist pitch  $\lambda$  of the wires is chosen to be equal to the arc length around a 90° bend on the cable ends with the bend radius  $R$  needed for the desired winding geometry:  $\lambda = \pi R/2$ . With this choice, all wires have the same catenary length around the bend, so no differential strain is produced within any wire.

Robotic bend tools (Fig. 7c) were developed with which saddle bends are formed in two stages: first a pair of 90° bends is formed into a U-bend with the spacing required for a given turn in the dipole winding, then the U-bend is bent 90° to form a flared end for the winding. Extensive experiments have

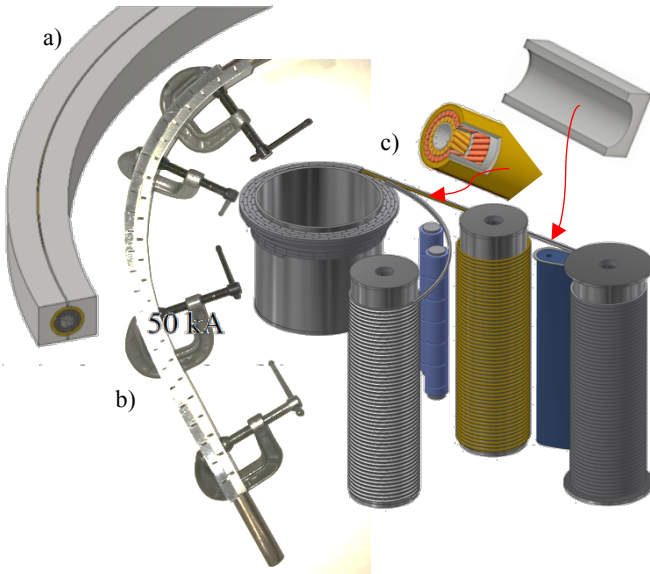


Fig. 8. Co-wound armor for SuperCIC: a) 2 half-shells of armor are co-wound with SuperCIC; b) actual prototype showing the pattern of kerf-cuts that accommodate bending the armor half-shells without deformation; c) configuration for coil-winding co-wound armored SuperCIC for a solenoid winding.

verified that, in a winding with formed ends with  $R = 5$  cm, there is no filament damage within the wires and the critical current of extracted wires is the same as that of witness wire samples [8].

SuperCIC was first developed for the windings of a superferic dipole for a proposed electron-ion collider [15]. For that application a single layer of NbTi wires was used. Two-layer SuperCIC is now being developed for the high-current, high-field requirements for future hadron colliders and for the solenoids and toroids of tokamaks. That has entailed process development for the choices of multi-layer over-wraps and sheath for a 30 kA cable, containing 40 wires:

- *NbTi SuperCIC* (Fig. 5b): it is critically important to interpose a multi-layer spiral wrap over-wrap that provides a slip-surface between inner and outer layers, and also a spiral over-wrap on the outer layer that provides a slip-surface. Those issues required a multi-layer over-wrap between wire layers.
- *2-layer Nb<sub>3</sub>Sn SuperCIC* (Fig. 5c): For Nb<sub>3</sub>Sn it was necessary to adopt proprietary materials for the slip-planes and sheath tube to provide the slip action during bending.
- *2-layer Bi-2212 SuperCIC* (Fig. 5d): multi-layer over-wrap foils are used to provide two distinct functions: Haynes 214 diffusion barrier foil prevents diffusion between wires and the center tube and sheath tube; slip-surface foils enable wires to re-arrange during coil forming. The sheath tube utilizes a proprietary superalloy that provides pressure containment during 880 C over-pressure (50 bar) heat treatment that is required to produce high-performance superconducting cores in the wire. By containing the high-temperature O<sub>2</sub>-Ar gas within the tube, there is no need to do heat treatment in a high-pressure furnace – a major simplification for coil technology.

ATC now manufactures single and double-layer SuperCIC cable in each of these superconducting wires in length up to 150 m as a commercial product.

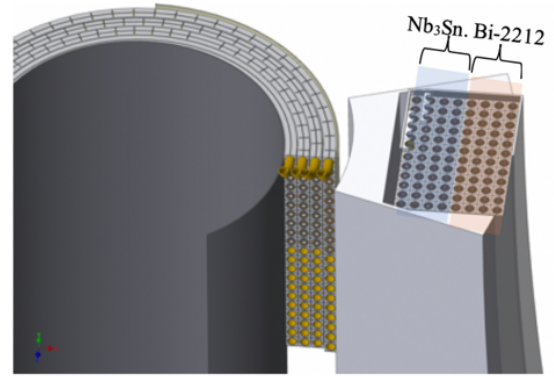


Fig. 9. Cross-sections showing the hybrid sub-windings for a solenoid and a toroid for the geometry of the tokamak of Fig. 3.

#### IV. LAYER-WOUND SUPERCIC FOR HYBRID WINDINGS

A strategic challenge to achieving high  $J_{WP}$  in a high-field toroid or solenoid arises from the dependence of critical current  $I_c$  in each superconductor upon the magnetic field at the conductor location. In either a solenoid or toroid, the background field on the winding closest to the interior is the highest anywhere; successive layers of the winding operate in successively lower background field, and the outermost layer operates in very little background field.

The three superconductors used in the winding designs presented here have dramatically different  $I_c(B)$  dependences – and also dramatically different cost [16]. NbTi has high  $I_c$  up to  $\sim 7$  T and wire costs \$2/m; Nb<sub>3</sub>Sn has high  $I_c$  up to  $\sim 14$  T and wire costs  $\sim$ \$7/m; Bi-2212/Ag has high  $I_c$  up to  $>40$  T, but costs  $\sim$ \$70/m. Thus to optimize both conductor cost and  $J_{WP}$ , it is essential to layer-wind the coil in a series of layers, and to utilize for each layer the least expensive superconductor that has high  $I_c$  at the background field that is present in that layer.

A second strategic challenge is to provide robust high-modulus support of the Lorentz stress that increases  $\sim$ linearly from the innermost layer of the winding to the outermost. In conventional CIC, the cable is inserted into a heavy-wall superalloy armor tube and the tube is drawn down onto the cable to compress it against the center tube. That approach typically deforms the wires and also leaves segments of wires unsupported within the ‘rope-of-ropes’ as discussed above. When the armor tube is then bent to form the winding, it deforms and the deformation is conveyed to the wires within.

A novel approach has been devised for the stress management of SuperCIC cables within a winding: a two-piece armor shell is co-wound with the SuperCIC. The configuration is shown in Fig. 8. Each armor half-shell has a half-square outer profile and a half-round inner profile. The inner profile is a snug fit to the SuperCIC, the outer profile provides a rib thickness that supports the transfer of radial stress from layer to layer, and a web thickness that supports the hoop stress in that layer of the winding.

Co-winding the half-shells presents its own challenge – how to prevent the side walls from deforming in a ‘crinkle’ when the half-shell is bent to a curve? For this we use an old carpenter’s trick: the side walls are slit on a regular spacing to

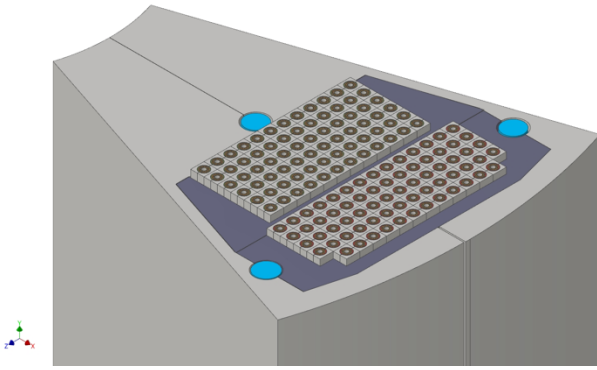


Fig. 10. Mid-plane cross section through one winding of a 16 T 10-sector toroid. SCHe coolant flow manifolds for cool-down are shown in blue.

form kerfs – cuts that extend to the bottom of the half-round inner profile, spaced so that when the half-shell is bent to a curve the half-shell bends at the kerf locations and does not inelastically strain either the web or the rib regions. Fig. 8b shows an actual prototype segment; Fig. 8c shows the configuration of supply spools and forming guides for co-winding.

We have developed an FEA model of the co-winding and verified that, for appropriate choice of the web, rib, and kerf, the armor retains most of its native modulus and the kerf slots just close at the top.

Fig. 9 shows cross-sections of a 12 T solenoid and a 16 T toroid for the spherical tokamak designed by PPPL.

## V. HYBRID WINDINGS - SUPERCIC AND CO-WOUND ARMOR

The SuperCIC conductor and co-wound armor provide a basis to subdivide windings into co-windings in which the superconductors in each are optimized for  $J_{WP}$  and total conductor cost. Fig. 10 shows an example of that optimization for the particular example of one module of a 16 T toroid. The winding is divided into an inner sub-winding of Bi-2212/Ag SuperCIC and an outer sub-winding of Nb<sub>3</sub>Sn/Cu SuperCIC.

Each sub-winding is layer-wound: each 12-turn layer is a single segment of SuperCIC ~150 m long, and successive layers are connected in electrical series by a demountable low-

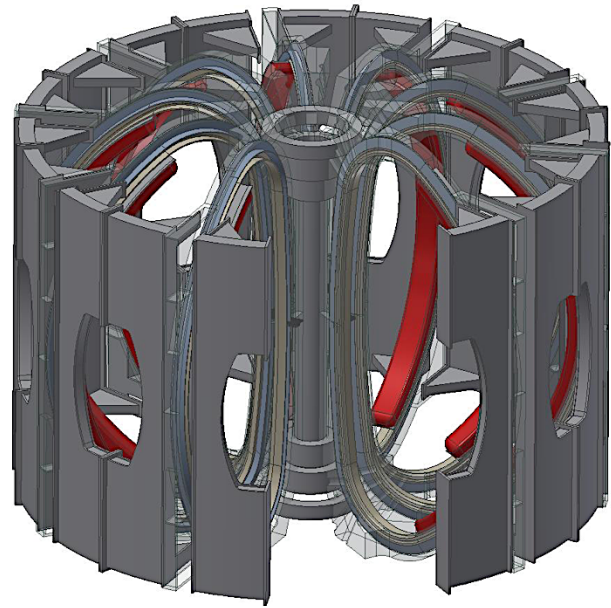


Fig. 12. Assembly of 10-sector 16 T toroid. One module has been removed to show inner structure.

resistance splice joints and in parallel for cryogen flow through the center tubes. Note that ATC has commissioned a complete SuperCIC fabrication facility capable of fabricating the required 150 m piece lengths (Fig. 6f).

The open geometry of the toroid makes it important to integrate a stress intercept between the two sub-windings: an overall stress shell supporting them as a unit, and a superstructure that ties all 10 windings into the overall toroid frame. Fig. 12 shows how this is accomplished for the SuperCIC windings.

Table I summarizes the main parameters of the 16 T toroid. Note that the superconductor cost is dominated by the cost of the superconducting wire. The wire costs shown in Table I are based on current small-quantity commercial quotations for present-day high-performance wire: Bi-2212 is \$13,800/kg for  $J_e = 1,500 \text{ A/mm}^2 @ 17 \text{ T}$ ; Nb<sub>3</sub>Sn is \$1,380/kg for  $J_e = 780 \text{ A/mm}^2 @ 12 \text{ T}$ . The total cost of superconductor is expensive, but does not dominate the total cost of such a tokamak. REBCO costs > 10x more, with comparable  $J_{WP}$  at best.

TABLE I  
MAIN PARAMETERS FOR HYBRID-WINDING 16 T TOROID.

$R_0$		1.2	m	
$B @ R_0$		6.7	T	
$B @ \text{coil}$		17.4	T	
$A$		2.0		
CIC	layers	#strands	Wire dia.	
	Bi-2212	5	42	0.97
	Nb <sub>3</sub> Sn	6	42	0.97
$J_{WP}$			140	MA/mm <sup>2</sup>
$I_{op}$			28.7	kA
$I_{op}/I_c @ 4.2K$			0.7	
Temperature margin			4.2-7	K
Quantity/cost of SC				
	Bi-2212	2.25 tons	\$5 M	
	Nb <sub>3</sub> Sn	1.9 tons	\$3 M	

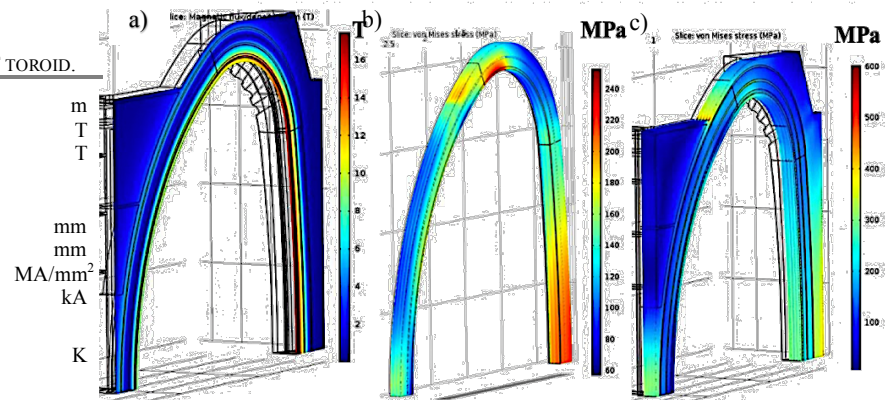


Fig. 11. a) Calculated field distribution in a sector of the 16 T toroid; b) von Mises stress distribution in the co-wound armor of the winding; c) von Mises stress distribution in the support structure of the winding module.

TABLE II.  
SCHE CRYOGENICS IN EACH LAYER OF A TOROID MODULE.

Heat load/bore	1	W/m
SCHe flow	0.3	m/s
Temperature rise	0.3	K
Pressure drop	0.8	bar
PdV work	0.03	W

Fig. 12a shows the calculated magnetic field distribution within the 16 T toroid winding. Fig. 12 shows the FEA simulation of the von Mises stress distribution in the co-wound armor within the winding package. It does not exceed the working strength of the super-alloy armor.

The maximum stress on the SuperCIC conductors is everywhere <120 MPa, which is below the threshold for strain degradation of the superconducting wires. This returns us to a primary motivation of the SuperCIC – to manage Lorentz stress so that all superconducting wires can operate with their full performance at the design field of the magnet.

## VI. CRYOGENICS, INSULATION, AND SPLICE JOINTS

The SuperCIC is designed to operate with Supercritical He (SCHe) flowing through the center tube. SCHe flow is connected in parallel through each layer of each sub-winding. Table II summarizes the parameters for flow, pressure, and temperature through the 150 m-long SuperCIC segment. The design accommodates a heat load of up to 10 W/layer (100 W/winding module) with a temperature swing of 0.3 K.

ATC and TAMU have developed a proprietary insulation technology that integrates with the forming of the co-wound armor and provides robust electrical insulation turn-turn and inter-layer.

ATC and TAMU have developed a proprietary demountable splice joint that joins the 42 wires of a 2-layer CIC to a sandwich of Rutherford cables with  $\sim n\Omega$  joint resistance. This development enables interconnection of the layers within the hybrid winding, and splices to supply bus-work. It also has the potential to make possible the fabrication of each toroid

winding module with separable inner and outer halves, so that each winding module could be assembled around a plasma vessel as is the case for NSTX and ITER.

## VII. CONCLUSION

SuperCIC windings brings several innovations to high-field magnetics for fusion systems:

- The SuperCIC manages stress at the cable level, so the huge accumulated Lorentz forces within windings cannot degrade fragile filaments of high-field superconductors. Round-profile SuperCIC makes it possible to integrate the cylindrical sheath and high-strength support elements as separate ingredients.
- The SuperCIC windings can be formed with small radius of curvature without harm to the wire or cable. It therefore provides a basis for high-field, small-radius solenoids, flexibility in reducing the aspect ratio of toroid windings, and challenging configurations for poloidal windings.
- SuperCIC supports hybrid coil strategies, in which sub-windings of different high-field conductors can be separately fabricated and heat-treated and then assembled as a winding.
- SuperCIC with Bi-2212 can be fabricated with provisions for sheath tube and over-wrap metals for which the sheath tube can serve as the pressure retort for over-pressure processing (no high-pressure furnace required).
- SuperCIC can be co-wound with a 2-piece armor shell that provides robust management of radial and hoop stress.
- Cryogen flow within SuperCIC distributes cooling throughout the volume of the winding, so that the variation in winding temperature from non-uniform heat loads is suppressed.

TAMU, ATC, and PPPL are collaborating to develop conceptual designs utilizing SuperCIC for the solenoid and toroid windings for an optimized spherical tokamak.

## VIII. REFERENCES

- [1] B. Bigot *et al.*, ‘Progress toward ITER’s first plasma’, Nucl. Fusion **59**, 112001 (2019).
- [2] P. Batistoni *et al.*, ‘The JET technology program in support of ITER’, Fusion Eng. and Design **89**, 896 (2014). <https://www.sciencedirect.com/science/article/abs/pii/S0920379613007643>
- [3] V.V. Postupaev *et al.*, ‘Results of the first plasma campaign in a start configuration of GOL-NB multiple-mirror trap’, Plasma Physics & Controlled Fusion **62**, 025008 (2020). <https://iopscience.iop.org/article/10.1088/1361-6587/ab53c2>
- [4] K. Risse *et al.*, ‘The magnet system of Wendelstein 7-X stellarator in operation’ Fusion Eng. and Design **136**, 12 (2018). <https://www.sciencedirect.com/science/article/pii/S0920379617309602>
- [5] Tokamak Energy, <https://www.tokamakenergy.co.uk/>
- [6] Commonwealth Fusion Systems <https://cfs.energy/>
- [7] T.J. Maguire, ‘Compact Fusion Reactor’, [https://arpa-e.energy.gov/sites/default/files/10\\_MCGUIRE.pdf](https://arpa-e.energy.gov/sites/default/files/10_MCGUIRE.pdf) (2017).
- [8] D. van der Laan, J. Weiss, and D. McRae, ‘Recent CORC progress’, Proc. Intl. Conf. on Cryogenic Materials, Hartford, July 21-25, 2019.
- [9] J.E. Menard, ‘Compact steady-state tokamak performance dependence on magnet and core physics limits’, Phil. Trans. R. Soc. A **377**, 20170440 (2019). <https://royalsocietypublishing.org/doi/full/10.1098/rsta.2017.0440?af=R>
- [10] T.G. Brown *et al.*, ‘A toroidal confinement facility study and eventual experimental device to investigate a range of liquid metal diverter and first wall concepts’, Proc. 27<sup>th</sup> Fusion Energy Conf., Gandhinagar(2018). [https://conferences.iaea.org/indico/event/151/papers/5878/files/4886-FEC-2018\\_-\\_FIP-P7-38\\_-\\_TBrown.pdf](https://conferences.iaea.org/indico/event/151/papers/5878/files/4886-FEC-2018_-_FIP-P7-38_-_TBrown.pdf)
- [11] J. Qin *et al.*, ‘New design of cable-in-conduit conductor for application in future fusion reactors’, Superconduct. Sci. and Tech. **30**, 115012 (2017). DOI: 10.1088/1361-6668/aa8900
- [12] A Vostner *et al.*, ‘Statistical analysis of the Nb3Sn strand production for the ITER toroidal field coils’, Supercond. Sci. Technol. **30** 045004 (2017). <https://doi.org/10.1088/1361-6668/aa5954>.
- [13] H.S. Kim *et al.*, ‘Measurement of a conduction cooled Nb<sub>3</sub>Sn racetrack coil’, IOP Conf. Series: Mat. Sci. and Eng. **279**,012018 (2017). DOI: doi:10.1088/1757-899X/279/1/012018
- [14] D. Chavez *et al.*, ‘Cable-in-Conduit using MgB<sub>2</sub>, Nb<sub>3</sub>Sn and Bi-2212 for wind-and-react coils’, Proc. Appl. Superconduct. Conf., Seattle, Oct. 28-Nov.2, 2018.
- [15] P.M. McIntyre *et al.*, ‘Cable-in-conduit dipoles for the Ion Ring of JLEIC’, IEEE Trans. Appl. Superconduct. **29**, 5, 4004806 <https://ieeexplore.ieee.org/iel7/77/6353170/08675432.pdf>

- 
- [16] P. Lee, *Engineering current density vs. field for practical superconductors*.  
[https://fs.magnet.fsu.edu/~lee/plot/Je\\_vs\\_B-041118\\_1280x929\\_PAL.png](https://fs.magnet.fsu.edu/~lee/plot/Je_vs_B-041118_1280x929_PAL.png)